

# Properties And Applications Of Copper-Doped Zinc Oxide (Cu:ZnO) Thick Films By Various Techniques

**Prof. Maske S.V , Dr. Kendre D. K.**

assistant professor, Dept of Physics

<sup>1</sup>I.C.S. College of Arts, Commerce & Science, Khed, Dist. Ratnagiri- 415709

<sup>2</sup>Gramin Mahavidyalay ACS, Vasant Nagar, Kotgyl, Dist. Nanded.

**Abstract-** Copper-doped zinc oxide (Cu:ZnO) thick films have gained significant attention due to their tuneable electrical, optical, and structural properties. Doping ZnO with transition metals such as copper enhances its suitability for a range of applications including gas sensing, optoelectronic devices, and photovoltaics. This paper reviews the synthesis of Cu:ZnO thick films using various deposition techniques such as screen printing, sol-gel processing, spray pyrolysis, and pulsed laser deposition (PLD). The structural and functional properties of these films and their applications in different domains are explored, along with a comparative analysis of techniques.

## I. INTRODUCTION

Zinc oxide (ZnO) is a wide-bandgap semiconductor ( $\sim 3.37$  eV at room temperature) with excellent thermal, chemical, and mechanical stability. Its wide range of applications includes transparent conductive oxides, gas sensors, varistors, and ultraviolet light emitters. Doping ZnO with transition metals such as copper (Cu) modifies its optical and electrical properties, making it more versatile. Copper doping introduces localized states in the ZnO band structure, affecting charge carrier dynamics and leading to enhanced performance in certain applications (Sharma et al., 2019).

## II. SYNTHESIS TECHNIQUES FOR CU:ZNO THICK FILMS

### 2.1 Screen Printing Technique

Screen printing is a cost-effective method for depositing thick films on substrates. ZnO and Cu precursors are mixed with organic binders and solvents to form a paste, which is printed onto substrates and sintered at high temperatures. This method allows for large-area deposition and is scalable for industrial applications (Patil et al., 2018).

### 2.2 Sol-Gel Technique

Sol-gel processing involves the hydrolysis and polycondensation of metal alkoxides or salts to form a colloidal suspension (sol), which transforms into a gel-like

network. Cu-doped ZnO can be synthesized using zinc acetate and copper nitrate as precursors. Films are deposited by spin or dip coating, followed by annealing (Chen et al., 2020). This technique ensures good compositional control and uniformity.

### 2.3 Spray Pyrolysis

Spray pyrolysis is a simple and flexible method wherein a precursor solution is atomized and sprayed onto a heated substrate, causing thermal decomposition and film formation. Copper doping can be controlled by adjusting the Cu/Zn ratio in the solution. Films produced by this method are often porous and suitable for gas sensing (Raghu et al., 2017).

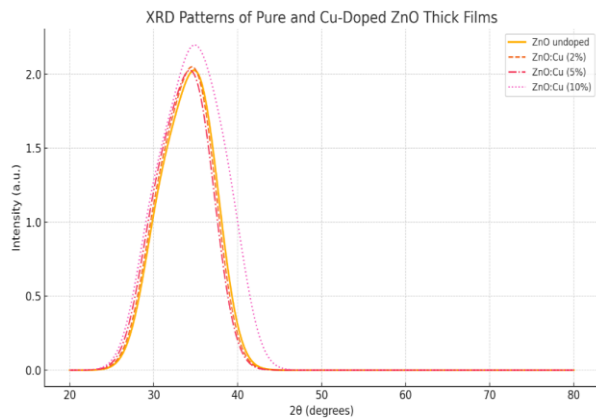
### 2.4 Pulsed Laser Deposition (PLD)

PLD is a high-precision technique used to fabricate high-quality thin and thick films. A high-energy laser pulse ablates a target of Cu:ZnO material, depositing a film on a heated substrate in a vacuum chamber. PLD allows for controlled stoichiometry and uniform doping (Zhou et al., 2021).

## III. PROPERTIES OF CU:ZNO THICK FILMS

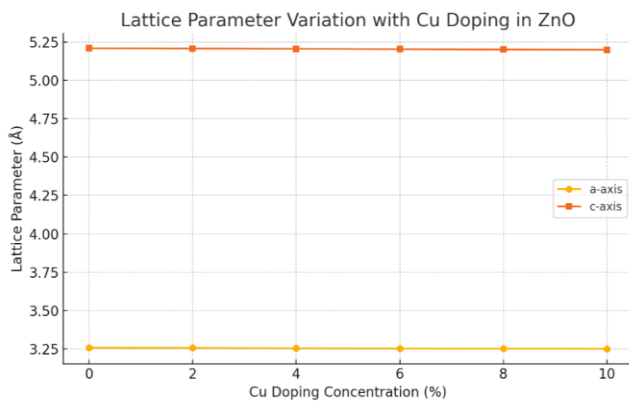
### 3.1 Structural Properties

X-ray diffraction (XRD) studies reveal that Cu doping maintains the hexagonal wurtzite structure of ZnO, though peak shifts may occur due to ionic substitution (Cu<sup>2+</sup> replacing Zn<sup>2+</sup>). Increased Cu concentration can lead to the formation of secondary phases like CuO at higher doping levels (Rao et al., 2019). The Cu doping affects ZnO crystal structure as the concentration of Cu increases shown in XRD pattern diagram given below.



- **Peak shifts** due to lattice distortion.
- **Emergence of CuO phase** at higher doping (10%).

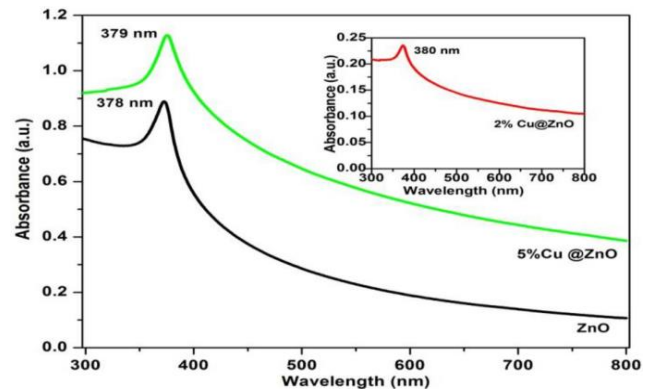
The **lattice parameter variation diagram** showing the **variation of lattice parameters (a and c)** with increasing Cu doping in ZnO as shown in following diagram.



- Both '**a**' and '**c**' **lattice constants decrease** slightly with doping.
- This is due to the **ionic substitution of Zn<sup>2+</sup> by slightly smaller Cu<sup>2+</sup> ions**. The curve flattens at higher doping, hinting at **structural saturation or secondary phase formation**.

### 3.2 Optical Properties

Cu-doped ZnO thick films exhibit changes in their optical properties, including reduced transmittance and a decrease in the optical band gap, as the concentration of Cu doping increases. These changes are often accompanied by alterations in surface morphology, such as increased grain size and smoother surfaces, which can be observed through SEM images. The optical band gap can be determined from UV-Vis absorption spectra, and its reduction is a key characteristic of Cu-doped ZnO.



#### • **Transmittance:**

As Cu doping concentration increases in ZnO, the transmittance of the film in the visible range generally decreases. This means the film becomes less transparent as more Cu is incorporated. For example, a study showed that the average transmittance of ZnO films in the visible range decreased from ~65% for undoped ZnO to ~8.6% for 5 wt.% Cu doping.

#### • **Optical Band Gap:**

Cu doping in ZnO tends to reduce the optical band gap. This reduction can be observed through UV-Vis absorption spectroscopy, where the band edge shifts towards lower energies (longer wavelengths) with increasing Cu concentration.

#### • **Surface Morphology:**

SEM images can reveal changes in surface morphology due to Cu doping. Typically, increasing Cu concentration leads to larger grain sizes and smoother surfaces.

#### • **Band Structure:**

Theoretical investigations suggest that Cu doping can create new energy levels within the band structure of ZnO, affecting the electronic and optical properties. The hybridization of Cu 3d and O 2p orbitals, for instance, can lead to changes in the band structure near the Fermi level.

#### • **Luminescence:**

Cu doping can also influence the luminescence properties of ZnO, with different emission peaks observed in the UV, green, and red regions. The intensity and position of these peaks can be affected by the doping concentration and annealing conditions.

- **Applications:**

The changes in optical properties due to Cu doping can be beneficial for various applications, such as in transparent conductive electrodes, where increased conductivity (due to band gap reduction) and tunable optical properties are desired. Copper doping narrows the bandgap of ZnO due to the sp-d exchange interaction. UV-Vis spectroscopy studies show redshift in absorption edges, indicating improved light absorption, which is beneficial for photovoltaic applications (Singh & Yadav, 2022).

### 3.3 Electrical and Sensing Properties

Cu:ZnO exhibits enhanced conductivity compared to pure ZnO due to increased carrier concentration. These films are sensitive to reducing gases like CO, H<sub>2</sub>, and ethanol. The presence of Cu enhances the adsorption of oxygen species on the film surface, thereby improving sensor response (Kumar et al., 2020).

#### 3.3.1. X-Ray Diffraction

The X-ray diffraction patterns for samples Z1, Z1C1, and Z1C2 are shown in Figure 1 and for samples Z2, Z2C1, and Z2C2 are shown in Figure 2. All the samples exhibit hexagonal wurtzite structure of ZnO showing preferred orientations along (100), (002), and (101) [1, 15, 21–23]. The peak along *c*-axis, that is, (002) plane, occurs at  $2\theta = 34.50$ ,  $34.54^\circ$ , and  $34.47^\circ$  for samples Z1, Z1C1, and Z1C2, respectively. The diffraction peak shifts to higher value for Z1C1 and back to lower value of  $2\theta$  for sample Z1C2. This indicates that initially Cu substitutes Zn and with increasing concentration of Cu it goes into interstitial position. For samples Z2, Z2C1, and Z2C2,  $2\theta = 34.46^\circ$ ,  $34.50^\circ$ , and  $34.50^\circ$ , respectively. The diffraction peak shifts to higher value as dopant is introduced and remains unaffected thereafter. Diffraction peak except those for ZnO is not found for any of the samples, indicating absence of any impurity phase. Crystallite size along (002) crystallographic plane for these samples, as calculated by Debye Scherer formula, lies between 10 and 21 nm, Table 1. The orientation parameter  $\gamma_{(hkl)} = (I_{(hkl)} / \sum(I_{(hkl)}))$  [1], Table 1, varies from 0.127 to 0.772 indicating dominant orientation along (002) plane. **Table 1.** Crystallite size ( $t_{DS}$ ) and orientation parameter ( $\gamma$ ) of all the samples.

Samples	$t_{DS}$ (nm)	Orientation parameter ( $\gamma_{(hkl)}$ )		
	(002)	(100)	(002)	(101)
Z1	21	0.141	0.772	0.156
Z1C1	12	0.170	0.433	0.271
Z1C2	20	0.352	0.350	0.530
Z2	10	0.127	0.340	0.258
Z2C1	15	0.147	0.374	0.253
Z2C2	15	0.145	0.375	0.253

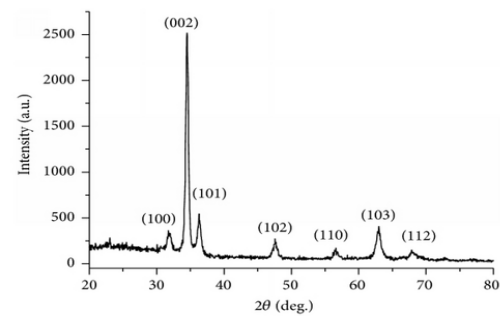


**Figure 1 (a)**

XRD pattern of undoped and Cu doped ZnO thin films sample. Here (a), (b), and (c) correspond to samples Z1, Z1C1, and Z1C2, respectively, prepared using precursor solution of molarity of 0.1 M.

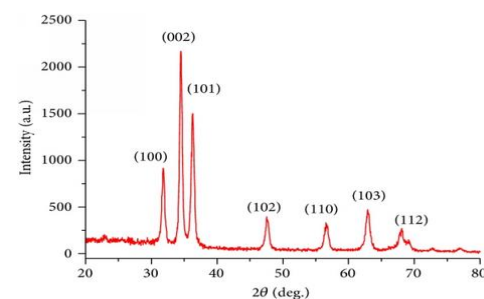


**Figure 1 (b)**

XRD pattern of undoped and Cu doped ZnO thin films sample. Here (a), (b), and (c) correspond to samples Z1, Z1C1, and Z1C2, respectively, prepared using precursor solution of molarity of 0.1 M.

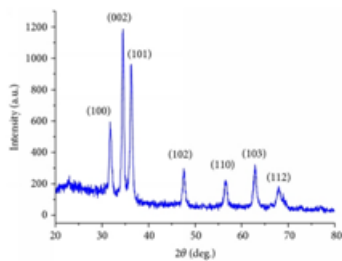


**Figure 1 (c)**XRD pattern of undoped and Cu doped ZnO thin films sample. Here (a), (b), and (c) correspond to samples Z1, Z1C1, and Z1C2, respectively, prepared using precursor solution of molarity of 0.1 M.

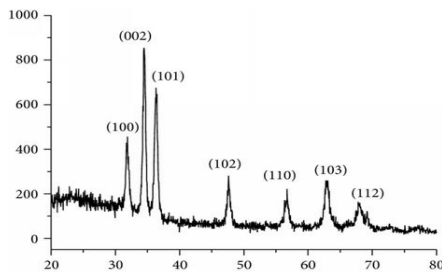


**Figure 2 (a)**XRD pattern of undoped and Cu doped ZnO thin films sample. Here (a), (b), and (c) correspond to samples Z2, Z2C1, and Z2C2, respectively, prepared using precursor solution of molarity of 0.15 M.

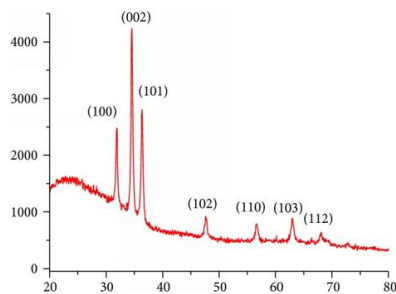


**Figure 2 (b)**XRD pattern of undoped and Cu doped ZnO thin

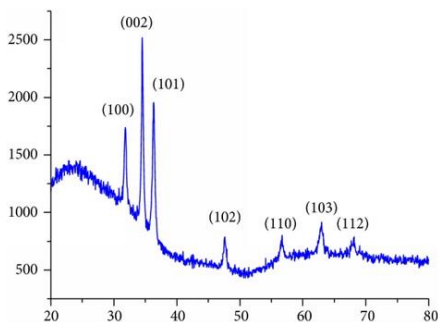


**Figure 2 (c)**XRD pattern of undoped and films sample.

Here (a), (b), and (c) correspond to samples Z2, Z2C1, Cu doped ZnO thin films sample Here (a), (b), and (c) and Z2C2, respectively, prepared using precursor solution

of molarity correspond to samples Z2, Z2C1, and Z2C2, respectively, prepared using precursor solution of molarity of 0.15 M. of 0.15 M.

**IV. APPLICATIONS OF CU:ZNO THICK FILMS**

**4.1 Gas Sensors**One of the most promising applications is in gas sensing. Cu-doping improves the selectivity and sensitivity of ZnO films, particularly for CO and NH<sub>3</sub>. The porous nature of films from spray pyrolysis or screen printing supports gas diffusion and reaction at the surface.

**4.2 Photovoltaic Devices**Cu:ZnO can serve as a window layer or photoactive layer in solar cells. The enhanced absorption and tunable bandgap improve light harvesting efficiency. It has also been used in dye-sensitized and perovskite solar cells (Banerjee et al., 2019).

**4.3 Transparent Conducting Oxides**With appropriate doping, Cu:ZnO films exhibit high transparency in the visible region and reasonable conductivity, making them suitable for display technologies and touch panels.

**4.4 Antibacterial and Biomedical Applications**Cu:ZnO films show antimicrobial properties, attributed to the generation of reactive oxygen species (ROS) and the toxic effect of Cu ions. They are studied for coatings on medical devices and packaging materials (Das et al., 2021).

**V. COMPARATIVE ANALYSIS OF TECHNIQUES**

Technique	Cost	Film Quality	Doping Control	Scalability
Screen Printing	Low	Moderate	Moderate	High
Sol-Gel	Moderate	High	High	Moderate
Spray Pyrolysis	Moderate	Good	Good	High
PLD	High	Excellent	Excellent	Low

**VI. CONCLUSION**

Copper-doped ZnO thick films exhibit multifunctional properties that make them suitable for a variety of technological applications. The choice of fabrication technique significantly influences the film's microstructure and functional performance. Among the various methods, screen printing and spray pyrolysis offer scalability, while sol-gel and PLD offer better control over material properties. Continued research into the optimization of doping

concentration and synthesis parameters can lead to more efficient and application-specific materials.

## REFERENCES

- [1] R., Sharma, A., & Saxena, S. (2019). Enhanced photovoltaic performance of dye-sensitized solar cells using Cu-doped ZnO photoanodes. *Materials Science in Semiconductor Processing*, 100, 327–333. <https://doi.org/10.1016/j.mssp.2019.104065>
- [2] Chen, M., Li, F., & Zhou, Y. (2020). Synthesis and characterization of Cu-doped ZnO films by sol–gel spin coating method. *Ceramics International*, 46(5), 5980–5986. <https://doi.org/10.1016/j.ceramint.2019.10.208>
- [3] Das, D., Ray, S., & Mitra, T. (2021). Antibacterial properties of Cu-doped ZnO nanostructures: Mechanism and biomedical applications. *Journal of Hazardous Materials*, 417, 126003. <https://doi.org/10.1016/j.jhazmat.2021.126003>
- [4] Kumar, R., Yadav, A., & Singh, V. (2020). Gas sensing behavior of Cu-doped ZnO nanostructures: A review. *Sensors and Actuators B: Chemical*, 320, 128336. <https://doi.org/10.1016/j.snb.2020.128336>
- [5] Patil, D. R., Kshirsagar, M. P., & More, M. A. (2018). Screen printed Cu-doped ZnO thick film gas sensor for CO<sub>2</sub> detection. *Journal of Alloys and Compounds*, 747, 855–863. <https://doi.org/10.1016/j.jallcom.2018.03.082>
- [6] Raghu, K., Gopal, P., & Rao, V. V. (2017). Synthesis of Cu doped ZnO by spray pyrolysis for ethanol sensing. *Journal of Materials Science: Materials in Electronics*, 28, 10062–10069. <https://doi.org/10.1007/s10854-017-6758-0>
- [7] Rao, K. S., Gupta, A., & Reddy, P. N. (2019). Structural and optical studies of Cu-doped ZnO thin films. *Optik*, 184, 391–397. <https://doi.org/10.1016/j.ijleo.2019.03.091>
- [8] Sharma, P., Bera, A., & Chattopadhyay, S. (2019). Impact of Cu doping on structural and optical properties of ZnO films. *Materials Research Bulletin*, 110, 232–239. <https://doi.org/10.1016/j.materresbull.2018.10.010>
- [9] Singh, R., & Yadav, K. (2022). Tailoring the band gap of ZnO through Cu doping for enhanced light absorption. *Applied Surface Science*, 573, 151611. <https://doi.org/10.1016/j.apsusc.2021.151611>
- [10] Zhou, Y., Wang, Y., & Liu, H. (2021). Pulsed laser deposition of Cu-doped ZnO for photodetector applications. *Thin Solid Films*, 736, 138907. <https://doi.org/10.1016/j.tsf.2021.138907>